THE JOURNAL OF BIOLOGICAL CHEMISTRY VOL. 291, NO. 9, pp. 4268–4280, February 26, 2016

The E3 Ubiquitin Ligase Adaptor Protein Skp1 Is Glycosylated by an Evolutionarily Conserved Pathway That Regulates Protist Growth and Development*[S]◆

Received for publication, November 11, 2015, and in revised form, December 19, 2015 Published, JBC Papers in Press, December 30, 2015, DOI 10.1074/jbc.M115.703751

Kazi Rahman[‡§¶], Peng Zhao[§‖], Msano Mandalasi[‡§], Hanke van der Wel[‡§], Lance Wells[§‖], Ira J. Blader[¶], and Christopher M. West[‡§1]**

*From the Departments of [‡]Biochemistry and Molecular Biology, University of Oklahoma Health Sciences Center, Oklahoma City, Oklahoma 73104, the [§]Department of Biochemistry and Molecular Biology, University of Georgia, Athens, Georgia 30602, the [¶]Department of Microbiology and Immunology, University of Oklahoma Health Sciences Center, Oklahoma City, Oklahoma 73104, the [‖]Complex Carbohydrate Research Center, Athens, Georgia 30602, and the **Department of Microbiology and Immunology, University at Buffalo, Buffalo, New York 14214*

Toxoplasma gondii **is a protist parasite of warm-blooded animals that causes disease by proliferating intracellularly in muscle and the central nervous system. Previous studies showed that a prolyl 4-hydroxylase related to animal HIFα prolyl hydroxylases is required for optimal parasite proliferation, especially at low O_2. We also observed that Pro-154 of Skp1, a subunit of the Skp1/Cullin-1/F-box protein (SCF)-class of E3-ubiquitin ligases, is a natural substrate of this enzyme. In an unrelated protist, *Dictyostelium discoideum*, Skp1 hydroxyproline is modified by five sugars via the action of three glycosyltransferases, Gnt1, PgtA, and AgtA, which are required for optimal O_2-dependent development. We show here that TgSkp1 hydroxyproline is modified by a similar pentasaccharide, based on mass spectrometry, and that assembly of the first three sugars is dependent on *Toxoplasma* homologs of Gnt1 and PgtA. Reconstitution of the glycosyltransferase reactions in extracts with radioactive sugar nucleotide substrates and appropriate Skp1 glycoforms, followed by chromatographic analysis of acid hydrolysates of the reaction products, confirmed the predicted sugar identities as GlcNAc, Gal, and Fuc. Disruptions of *gnt1* or *pgtA* resulted in decreased parasite growth. Off target effects were excluded based on restoration of the normal glycan chain and growth upon genetic complementation. By analogy to *Dictyostelium* Skp1, the mechanism may involve regulation of assembly of the SCF complex. Understanding the mechanism of *Toxoplasma* Skp1 glycosylation is expected to help develop it as a drug target for control of the pathogen, as the glycosyltransferases are absent from mammalian hosts.**

Toxoplasma is a worldwide obligate intracellular apicomplexan parasite that infects most nucleated cells of warm-blooded animals (1). Toxoplasmosis, the disease caused by *Toxoplasma*, is an opportunistic infection in AIDS and other immune-suppressed patients (2). In addition, *in utero* infections can cause mental retardation, blindness, and death (3). *Toxoplasma* is transmitted by digesting parasites from feline feces (as oocysts) or undercooked meat (as tissue cysts). Once in the host, parasites convert to the tachyzoite form that disseminates to peripheral tissues (*e.g.* brain, retina, and muscle). The resulting immune response and/or drugs can control tachyzoite replication, but the parasite survives by converting into slow growing bradyzoites that encyst. Cysts sporadically burst, and the released parasites convert to tachyzoites whose unabated growth, as can occur in immune suppressed hosts, results in cell and tissue damage (4). Currently, no *Toxoplasma* vaccine exists; anti-toxoplasmosis drugs have severe side effects, and resistance to these drugs is occurring.

Recently, disruption of the gene for PhyA, the prolyl 4-hydroxylase that hydroxylates Pro-154 in Skp1, was observed to reduce tachyzoite proliferation in cell culture and fitness in a competition assay (5). Skp1 is an adaptor in the Skp1/Cullin-1/F-box protein (SCF)[2] class of E3 ubiquitin ligases, and its hydroxylation was hypothesized to contribute to O_2-dependent proliferation. That study noted that loss of hydroxylation resulted in increased migration in SDS-polyacrylamide gels suggesting a decrease in M_r of ~1000. Previous studies in an unrelated protist, the social soil amoeba *Dictyostelium*, had shown that the Skp1-hydroxyproline (Hyp) could be glycosylated by five glycosyltransferase activities encoded by three genes, resulting in assembly of a pentasaccharide at the equivalent Pro residue (6, 7). Because two of these genes, *gnt1* and *pgtA*, have apparent homologs in the *Toxoplasma* genome, we suspected that the gel shift might result from inability of the

* This work was supported in part by Grant 14-140 from the Mizutani Foundation for Glycoscience (to C. M. W. and I. J. B.), Oklahoma Center for the Advancement of Science and Technology Grant HR10-0181 (to C. M. W.), and National Institutes of Health Grants R01-GM084383 (to C. M. W. and I. J. B.) and R01-AI069986 (to I. J. B.). The authors declare that they have no conflicts of interest with the contents of this article. The content is solely the responsibility of the authors and does not necessarily represent the official views of the National Institutes of Health.

◆ This article was selected as a Paper of the Week.

[S] This article contains supplemental Table S1 and Figs. S1 and S2.

[1] To whom correspondence should be addressed. Tel.: 706-542-4259; E-mail: westcm@uga.edu

[2] The abbreviations used are: SCF, Skp1/Cullin-1/FBP subcomplex of the Cullin-1/RING ligase class of E3 ubiquitin ligases; GlcNAcT, polypeptide *N*-acetyl-α-glucosaminyltransferase; GT, glycosyltransferase; HFF, human foreskin fibroblast; Hyp, 4*R*,2*S*-(*trans*)-hydroxyproline; S100, cytosolic extract prepared as the supernatant after 100,000 × *g* centrifugation; SF-tag, a 51-amino acid peptide including 2 Strep-tag II epitopes and a FLAG epitope; CID, collision-induced dissociation; MPA, mycophenolic acid; dHex, deoxyhexose.

glycosyltransferases to modify Skp1 in the absence of formation of the Hyp anchor. In *Dictyostelium*, Dd*gnt1* encodes a polypeptide αGlcNAc transferase that transfers GlcNAc from UDP-GlcNAc to form GlcNAcα1-*O*-Skp1 (8). Dd*pgta* encodes a dual function diglycosyltransferase whose N-terminal domain then transfers Gal from UDP-Gal to form a Galβ1–3GlcNAc linkage and whose C-terminal domain processively transfers Fuc from GDP-Fuc to form a Fucα1–2Gal linkage (9). However, the two domains are switched in the *Toxoplasma* version of the predicted protein (TGGT1_260650), and there is no evidence for *agtA*, the *Dictyostelium* gene that is responsible for addition of the final two sugars, both αGal residues.

If the Skp1 Hyp of *Toxoplasma* can be glycosylated, the importance of hydroxylation for proliferation might be due to consequent loss of glycosylation rather than inability to hydroxylate *per se*. In *Dictyostelium*, hydroxylation alone partially rescues O_2-dependent development (10). Full recovery depends, however, on full glycosylation (11), and glycosylation is required to promote efficient assembly of the Skp1/F-box protein heterodimer, based on interactome studies (12). Therefore, we sought direct evidence for Hyp-dependent glycosylation of *Toxoplasma* Skp1 and the role of the predicted glycosyltransferases, and we used disruption strains of the predicted glycosyltransferase genes to test their contribution to parasite proliferation. The findings implicate Skp1 as the functional target of this novel post-translational modification pathway in *Toxoplasma* and indicate that the Skp1 modification pathway is evolutionarily conserved among protists.

Experimental Procedures

Parasites, Cell Culture, and Plaque Assays—*Toxoplasma* strain RHΔ*ku80*Δ*hxgprt* (RHΔΔ) was cultured in association with human foreskin fibroblasts (HFFs) using Dulbecco's modified Eagle's medium (DMEM) supplemented with 10% (v/v) fetal bovine serum, 2 mM L-glutamine, and 100 units/ml penicillin/streptomycin (Complete medium) in a humidified CO_2 (5%) incubator at 37 °C. RHΔ*ku80*Δ*phyA* (RH*phyA*Δ), RHΔ*ku80*Δ*gnt1* (RH*gnt1*Δ), and RHΔ*ku80*Δ*pgtA* (RH*pgtA*Δ) strains were cultured in the same medium supplemented with 25 μg/ml mycophenolic acid (Sigma) and 25 μg/ml xanthine (Sigma). RHΔ/SF and RH*phyA*Δ-1/SF strains, where TgSkp1 was tagged with the SF-tag and have the chloramphenicol acetyltransferase marker, were cultured in DMEM supplemented with 20 μM chloramphenicol (Sigma). Strains were cloned by limiting dilution in 96-well plates.

To perform cell growth plaque assays, confluent HFF monolayers in 6-well tissue culture plates were infected with freshly lysed-out (see below) parasites at 250 parasites/well, equivalent to a multiplicity of infection of 0.002. After 3 h, unattached parasites were removed by two rinses with phosphate-buffered saline (15 mM sodium phosphate, pH 7.4, 135 mM NaCl). After undisturbed incubation in Complete medium for 5.5 days, monolayers were fixed with methanol and stained with crystal violet to detect plaques. Plaques ($n \geq 50$) from at least two wells were manually encircled, and areas were calculated by ImageJ software (National Institutes of Health). Data were presented and statistically analyzed using GraphPad Prism version 6.

TgphyA, Tggnt1, and TgpgtA Disruption Strains—DNAs for gene disruptions were generated from pminiGFP.ht (gift of Dr. Gustavo Arrizabalaga, University of Idaho), in which the *hxgprt* gene is flanked by multiple cloning sites. The approach was modeled after that used for the Tg*phyA* disruption strain RH*phyA*Δ-1, in which exon 1 of Tg*phyA* was replaced with *hxgprt* (5). To generate an independent Tg*phyA* disruption strain, RH*phyA*Δ-2, the complete coding region was replaced with *hxgprt* by double crossover homologous recombination. First, the 5′- and 3′-flank targeting sequences of Tg*phyA* from RHΔΔ were PCR-amplified with primer pairs a and a′ and pairs b and b′, respectively (supplemental Table S1). The 5′-fragment was digested with KpnI and HindIII and inserted into pminiGFP.ht between its KpnI and HindIII sites. The resulting plasmid was digested with XbaI and NotI and ligated to the XbaI- and NotI-digested 3′-flank. The resulting vector was linearized with KpnI and electroporated into RHΔΔ strain as described (5). Drug-resistant transformants were selected in the presence of 25 μg/ml MPA and 25 μg/ml xanthine and cloned by limiting dilution. Genomic DNA from three clones was screened by PCR to identify Tg*phyA* disruption strain RH*PhyA*Δ*-2*, as described under "Results." The PCRs were performed on extracts from 2×10^6 parasites, using *Taq* polymerase, and primers as listed in supplemental Table S1. Standard conditions included 1.5 mM $MgCl_2$, and reactions were run for 30 cycles of the following standard scheme: 94 °C, 30 s; 60 °C, 1 min; 68 °C, 3 min. Exact conditions were adjusted for specific reactions.

To disrupt Tg*gnt1*, the 5′-flank and 3′-flank targeting sequences were PCR-amplified with primer pairs c and c′ and d and d′ (supplemental Table S1), respectively, and inserted into pminiGFP.ht as above. The vector was linearized with SapI and transfected into RHΔΔ, and drug-resistant clones were screened by PCR to generate the Tg*gnt1* disruption strain (RHg*nt1*Δ). Similarly, the Tg*pgtA* disruption construct was generated by PCR amplification and insertion into pminiGFP.ht of 5′-flank and 3′-flank targeting sequences using primer pairs e and e′ and f and f′, respectively. After digestion with PacI, the DNA was transfected into RHΔΔ, and RH*pgtA*Δ clones were screened by PCR.

Tggnt1 and TgpgtA Complemented Strains—pminiGFP.ht was used as the backbone for constructing the Tg*gnt1* complementation construct after removing its HXGPRT cassette by KpnI and NotI digestion. A 7-kb DNA fragment containing the Tg*gnt1* genomic region was PCR-amplified using primer pairs c and d′ (supplemental Table S1), digested with KpnI and NotI, and ligated into the similarly digested pminiGFP.ht. The resultant vector was linearized with KpnI and electroporated into RH*gnt1*Δ. Transformants were selected under 300 μg/ml 6-thioxanthine (Matrix Scientific), and clones were screened by PCR. To complement Tg*pgtA* knock-out, the fosmid clone Rfos01M21 (13), containing a 36-kb fragment of RH strain chromosome VIIb (2039542–2076165), which includes the Tg*pgtA* gene (gift of Dr. Boris Striepen, University of Georgia), was linearized with ScaI and electroporated into RH*pgtA*Δ. Complemented clones were isolated as described for Tg*gnt1*.

Epitope Tagging of Endogenous TgSkp1—To modify the C terminus of endogenous TgSkp1, the *skp1* genomic locus was

TABLE 1
***Toxoplasma* strains used in this study**

Strain	Parental strain	Genotype	Gene targeted	Selection marker	Selection drug	Ref.
KU80ΔΔ	RH(I)	Δku80;Δhxgprt				26
RHΔ*phyA*-1	KU80ΔΔ	*phyA*Δ;Δku80	*phyA*-exon 1	Hxgprt	MPA, xanthine	5
RHΔ*phyA*-2	KU80ΔΔ	*phyA*Δ;Δku80	*phyA*-exons 1–9 (all)	Hxgprt	MPA, xanthine	TR[a]
RHΔ*gnt1*	KU80ΔΔ	*gnt1*Δ;Δku80	*gnt1*-exon 1 (all)	Hxgprt	MPA, xanthine	TR
RHΔ*gnt1*/complemented	RHΔ*gnt1*	Δku80;Δhxgprt		ΔHxgprt	6-Thioxanthine	TR
RHΔ*pgtA*	KU80ΔΔ	*pgtA*Δ;Δku80	*pgtA*-exons 1–14 (all)	Hxgprt	MPA, xanthine	TR
RHΔ*pgtA*/complemented	RHΔ*pgtA*	Δku80;Δhxgprt		ΔHxgprt	6-Thioxanthine	TR
RHΔΔ/Skp1-SF	KU80ΔΔ	$Skp1^{SF}$;Δku80; Δhxgprt;CAT^{+}	Skp1 C-terminus	CAT	Chloramphenicol	TR
RHΔ*phyA*-1/Skp1-SF	RH*phyA*Δ-1	$Skp1^{SF}$;*phyA*Δ; Δku80;CAT^{+}	*phyA*-exon 1; Skp1 C terminus	CAT	Chloramphenicol	TR

[a] TR means this report.

modified by the insertion of SF-tag cDNA. A 1.5-kb region upstream of the *skp1* stop codon was PCR-amplified using primer pairs g and g′. Using a ligation-independent cloning strategy (14), the product was inserted into PacI-digested pSF-TAP-LIC-HXGPRT and pSF-TAP-LIC-CAT vectors (from Dr. Vern Carruthers, University of Michigan). 50 μg of the resulting constructs were linearized with EcoRV at position 527 of the insert, and the DNAs were electroporated into RHΔΔ and RH*phyA*Δ*-1*, respectively. RHΔ/SF transformants were selected under 25 μg/ml MPA/xanthine, and RH*phyA*Δ-1/SF was selected under 20 μM chloramphenicol. Site-specific integration was confirmed by PCR of clones using the primer pairs h and h′. DNA sequencing confirmed that the 3′-end of the Skp1 coding sequence encoded the native C terminus (. . . VREENKWCEDA) followed by a peptide containing two Strep-II tags and a FLAG tag (in boldface), *AKIGSGGR-EF**WSHPQFEK**GGGSGGGSGGGS**WSHPQFEK**GASGE**DYK-DDDDK***. Characteristics of the above strains are summarized in Table 1.

Purification of Endogenous TgSkp1—Tachyzoites from RHΔΔ, RH*phyA*Δ*-1*, RH*gnt1*Δ, and RH*pgtA*Δ strains were harvested from infected HFF monolayers by scraping and passage through a 27-gauge needle, centrifuged at 2000 × *g* for 8 min at room temperature, resuspended in sterile phosphate-buffered saline, and counted on a hemacytometer chamber as described (15). 6×10^8 tachyzoites were pelleted, frozen at −80 °C, and subsequently thawed and solubilized in 8 M urea, 50 mM HEPES-NaOH, pH 7.4, supplemented with protease inhibitors (1 mM PMSF, 10 μg/ml aprotinin and 10 μg/ml leupeptin) at 4 °C for 30 min. The lysates were centrifuged at 16,000 × *g* for 15 min at 4 °C, and supernatants (S16) were collected and diluted 8-fold in IP buffer (0.2% Nonidet P-40 (v/v) in 50 mM HEPES-NaOH, pH 7.4, protease inhibitors) and incubated with 60 μl of rabbit polyclonal anti-TgSkp1 UOK75-Sepharose beads for 1 h at 4 °C. The UOK75 antiserum (5) was first affinity-purified against recombinant TgSkp1-Sepharose beads, performed as described for affinity purification of anti-DdSkp1 (12), and then coupled to CNBr-activated Sepharose CL-4B. After centrifuging and resuspending the beads three times with IP buffer and three times with wash buffer (10 mM Tris-HCl, pH 7.5, 154 mM NaCl), bound material was eluted twice with 150 μl of 133 mM triethylamine, pH 11.5, for 10 min and immediately neutralized with 150 μl of 200 mM acetic acid, pH 2.7. The pooled eluates (~400 μl) were divided into two equal parts, concentrated by vacuum centrifugation to ~10 μl, and snap-frozen in liquid nitrogen. To purify SF-tagged TgSkp1, soluble S16 fractions were prepared from RHΔ/SF and RHp*hyA*Δ-1/SF strains as described above and incubated with 100 μl of mouse anti-FLAG M2-agarose beads (Sigma) for 1 h at 4 °C. The beads were washed as above and eluted with 300 μl of 8 M urea in 25 mM NH_4HCO_3 (natural pH), supplemented with 40 mg of urea, and incubated for 15 min at room temperature, and the supernatants harboring TgSkp1-SF were collected at 2400 × *g* for 5 min in room temperature.

Mass Spectrometry of TgSkp1 Peptides—The untagged TgSkp1 samples were taken to dryness and solubilized in 100 μl of 8 M urea in 25 mM NH_4HCO_3. The untagged and SF-tagged TgSkp1 samples were reduced by addition of 0.5 M tris(2-carboxyethyl-)phosphine to a final concentration of 5 mM for 20 min at 22 °C and alkylated by the addition of 0.5 M iodoacetamide to a final concentration of 10 mM for 15 min in the dark. Tris(2-carboxyethyl)phosphine was then added to a final concentration of 10 mM, and 300 μl of 50 mM NH_4HCO_3, pH 7.8, was added to dilute urea to 2 M. Samples were treated with 1 mg/ml mass spectrometry grade trypsin (Promega) at a final concentration 8.0 μg/ml and incubated overnight at 37 °C. Peptides were recovered by adsorption to a C18 Zip Tip (OMIX TIP C18 100 μl) and eluted with 0.1% trifluoroacetic acid in 50% (v/v) acetonitrile.

Dry peptides were reconstituted in 15.6 μl of solvent A (0.1% formic acid) and 0.4 μl of solvent B (0.1% formic acid in 80% acetonitrile) and loaded onto a 75-μm (inner diameter) × 115-mm C18 capillary column (YMC GEL ODS-AQ120ÅS-5, Waters) packed in-house with a nitrogen bomb. Peptides were eluted into the nanospray source of an LTQ Orbitrap™ mass spectrometer (Thermo Fisher Scientific) with a 160-min linear gradient consisting of 5–100% solvent B over 100 min at a flow rate of 250 nl/min. The spray voltage was set to 2.0 kV, and the temperature of the heated capillary was set to 210 °C. Full scan MS spectra were acquired from *m*/*z* 300 to 2000 at 30,000 resolution, and MS2 scans following collision-induced fragmentation were collected in the ion trap for the 12 most intense ions. The raw spectra were searched against a *Toxoplasma gondii* protein database (UniProt ATCC 50611/Me49, Sept. 2013) using SEQUEST (Proteome Discoverer 1.3, Thermo Fisher Scientific) with full MS peptide tolerance of 50 ppm and MS2 peptide fragment tolerance of 0.5 Da and filtered to generate a 1% target decoy peptide-spectrum-match false discovery rate for protein assignments. The spectra assigned as glycosylated TgSkp1 peptides were manually validated.

Cytosolic (S100) Extracts—Parasites were permeabilized as described (16) with slight modifications. Briefly, a pellet of 2.5×10^9 frozen tachyzoites was resuspended in 500 μl of ice-cold water containing 10 μg/ml aprotinin, 10 μg/ml leupeptin,

1 mM PMSF, and 0.1 mM *N*-α-*p*-tosyl-L-lysine chloromethyl ketone and incubated for 10 min on ice. The suspension was transferred to a Dounce homogenizer and sheared by 10 strokes, diluted with an equal volume of 100 mM HEPES-NaOH, pH 7.4, 10 mM $MgCl_2$, 10 mM $MnCl_2$, 50 mM KCl, 10 μg/ml aprotinin, 10 μg/ml leupeptin, 1 mM PMSF, and sheared by 20 additional strokes. After confirmation of lysis using phase contrast microscopy, the lysate was centrifuged at 200,000 × *g* at 5 °C for 35 min; the supernatant (S100) was immediately desalted over a PD10 column at 5 °C into 50 mM HEPES-NaOH, pH 7.4, 5 mM $MgCl_2$, 15% (v/v) glycerol, and 0.1 mM EDTA. Fractions with highest A_{280} values (≥1, 1-cm path length) were snap-frozen at −80 °C for enzyme assays.

Glycosyltransferase Assays—Skp1-dependent GlcNAcT activity was assayed in S100 fractions by the transfer of ^{3}H from UDP-[^{3}H]GlcNAc to exogenous *Dictyostelium* HO-DdSkp1 (17). Typically, a 50-μl reaction volume containing 30 μl of S100 fraction, 50 pmol of HO-DdSkp1 (18), and 0.5–2.5 μM UDP-GlcNAc (including 1 μCi of UDP-[^{3}H]GlcNAc at 37 Ci/mmol, PerkinElmer Life Sciences), in 50 mM HEPES-NaOH, pH 7.4, 10 mM $MgCl_2$, 2 mM DTT, 3 mM NaF, and protease inhibitors, was incubated at 30 °C for 0, 1, or 3 h. Reactions were stopped by addition of 4× Laemmli electrophoresis sample buffer, supplemented with 2 μg of soybean trypsin inhibitor (Sigma) as a marker that comigrates with DdSkp1, boiled for 5 min, and resolved by SDS-PAGE (see below). The gel was stained for 1 h with 0.25% (w/v) Coomassie Blue in 45% (v/v) methanol, destained overnight in 5% (v/v) methanol, 7.5% (v/v) acetic acid, and rinsed in H_2O for 1 h. Five ~1-mm gel slices including and surrounding the soybean trypsin inhibitor band were excised and incubated in 7 ml of a scintillation mixture containing 100 ml of Soluene-350 (PerkinElmer Life Sciences) and 900 ml of 0.6 g/liter 2,5-diphenyloxazole and 0.15 g/liter dimethyl-1,4-bis(4-methyl-5-phenyl-2-oxazoyl)benzene in scintillation grade toluene. After 5 days, ^{3}H was quantitated by scintillation counting in a Beckman LSC6500 instrument.

GalT activity was assayed similarly except that the donor was 1 μM UDP-[^{3}H]Gal and prepared from a mixture of 1 μCi of UDP-[^{3}H]Gal (7) and unlabeled UDP-Gal, and the acceptor was recombinantly prepared GlcNAc-DdSkp1 (18). FucT activity was similarly assayed except that 2 μM GDP-[^{3}H]Fuc, prepared from a mixture of GDP-[^{3}H]Fuc (1 μCi of 20 Ci/mmol, PerkinElmer Life Sciences) and unlabeled GDP-Fuc, was used in place of UDP-[^{3}H]Gal, and 2 μM unlabeled UDP-Gal was added to generate Gal-GlcNAc-DdSkp1 acceptor from the added GlcNAc-DdSkp1.

Radioactive Sugar Analyses—The chemical form of the radioactivity incorporated into DdSkp1 was determined by high pH anionic exchange chromatography analysis after acid hydrolysis as described (17). Briefly, Gnt1 reaction products were resolved by SDS-PAGE and electroblotted onto a 0.45-μm PVDF membrane (EMD Millipore). The membrane was stained with 0.2% Ponceau S in 3% (w/v) TCA, and the Skp1 protein band was excised with a razor blade, submerged in 400 μl of 6 M HCl, and incubated at 100 °C for 4 h. Hydrolysates were removed into microtubes, evaporated to dryness under vacuum centrifugation, dissolved in 500 μl of H_2O, dried again twice, and reconstituted in 25 μl of H_2O. A solution containing 1 nmol of $GalNH_2$ and $GlcNH_2$ in 9 μl of H_2O was added to the hydrolysates and chromatographed on PA-1 column on a DX-600 Dionex high pH anionic exchange chromatography workstation in 16 mM NaOH at 1 ml/min with pulsed amperometric detection. Fractions were collected into EconoSafe (Research Products International) scintillation fluid and counted for ^{3}H incorporation on a liquid scintillation counter. PgtA assay products were similarly hydrolyzed in 4 M TFA and mixed with a standard solution containing 1.5 nmol each of Glc, Gal, Man, and Fuc.

Western Blotting—Western blotting was performed as described (5). Briefly, tachyzoite pellets were solubilized in lysis buffer containing 8 M urea, 50 mM HEPES-NaOH, pH 7.4, supplemented with protease inhibitors at 4 °C for 30 min and centrifuged at 16,000 × *g* for 15 min at 4 °C to generate a soluble S16 fraction. After combining with SDS-PAGE sample buffer, proteins were resolved on a 4–12% gradient SDS-polyacrylamide gel (NuPAGE Novex, Invitrogen) and transferred to a nitrocellulose membrane using an iBlot system (Invitrogen). After probing with a 1:500-fold dilution of the UOK75 anti-TgSkp1 antibody and a 1:10,000-fold dilution of Alexa-680-labeled goat anti-rabbit IgG secondary antibody (Invitrogen), blots were imaged on a Li-Cor Odyssey infrared scanner.

Results

Toxoplasma Skp1 Is Modified by a Pentasaccharide—Our previous study showed that disruption of exon 1 of the Skp1 prolyl 4-hydroxylase gene (*phyA*) in the parental type 1 strain RHΔ*ku80*Δ*hxgprt* (RHΔΔ) resulted in greater mobility of Skp1 during SDS-PAGE, corresponding to an M_r difference of about 1000 (5). To investigate the possibility that this was due to a loss of hydroxylation-dependent glycosylation as occurs in *Dictyostelium* (6), a previously described antiserum raised against recombinant TgSkp1 (5) was used to immunoprecipitate Skp1 from tachyzoite extracts, and its tryptic peptides were analyzed by conventional nano-LC/MS in an LTQ-XL Orbitrap mass spectrometer. Peptides covering 75% of the 170-amino acid sequence of Skp1, including ^{145}IFNIVNDFT**P**EEEAQVR containing unmodified Pro-154 (*m*/*z* 1011, $[M + 2H]^{2+}$) eluting at 88.7 min, were observed. Potential hydroxylated glycopeptides were sought using a theoretical mass list of glycoforms of this peptide containing any combination of 1–8 residues of Hex, dHex, HexNAc, HexUA, and pentose. This search yielded, at 82.7 min elution time, a single glycopeptide ($[M + 2H]^{2+}$, 1437.1464; $[M + 3H]^{3+}$, 958.09) with an exact match (within 0.56 ppm) to a glycoform containing 1 HexNAc, 3 Hex, and 1 dHex residues (Fig. 1*A*). Similar results were obtained for a Skp1-SF preparation isolated by anti-FLAG immunoprecipitation from a strain in which Skp1 was C-terminally modified by an SF-tag (data not shown). The putative glycopeptide ion was absent from the RH*phyA*Δ strain (summarized in Table 2), consistent with its identity as the predicted Skp1 glycopeptide.

The putative glycopeptide ion was subjected to MS/MS analysis to confirm its composition and characterize its organization. Fragmentation of the doubly charged parent ion by CID yielded a series of ions whose mass differences corresponded to loss of a combination of Hex, dHex, and/or HexNAc residues (Fig. 1*B*), resulting ultimately in the expected hydroxypeptide

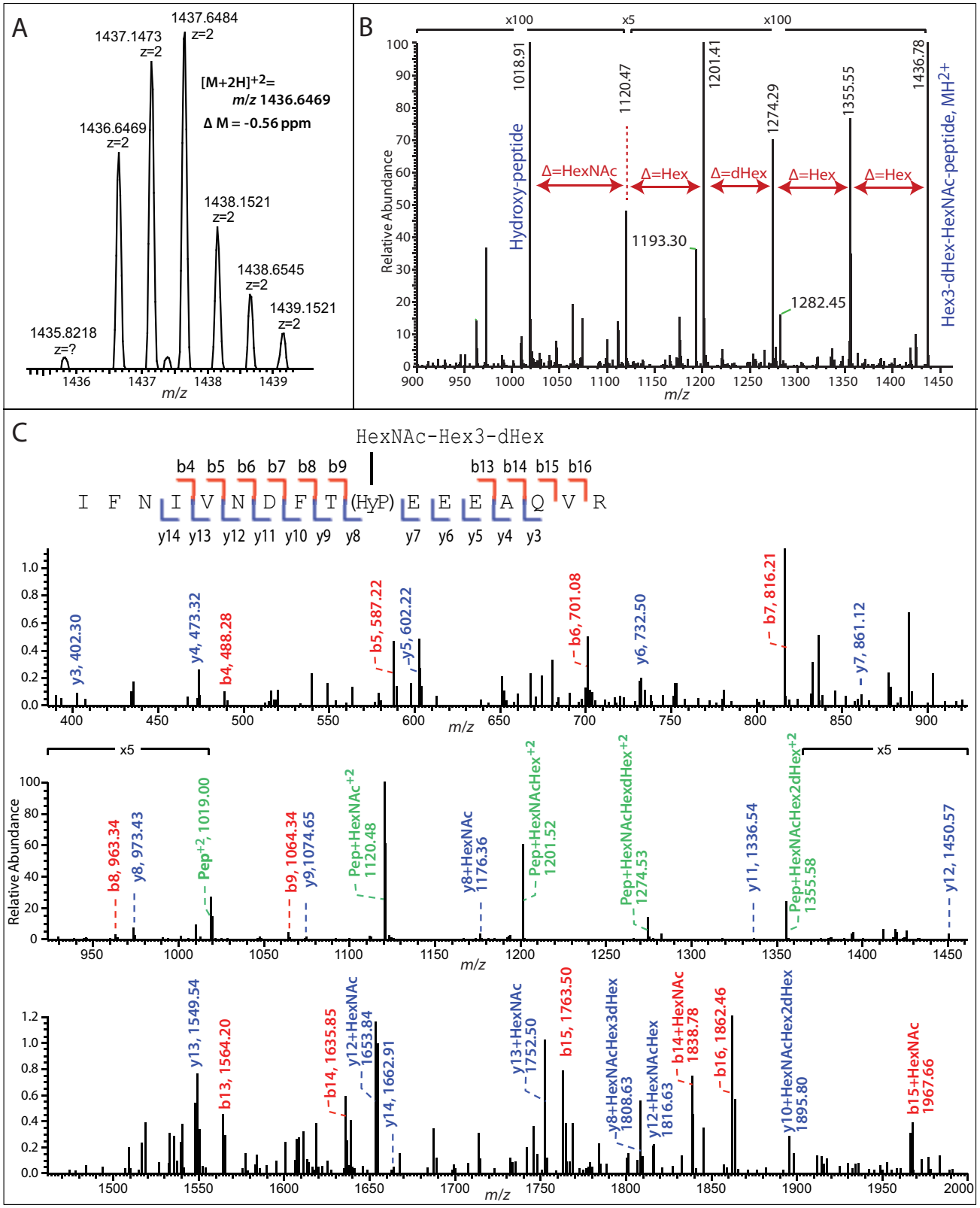

FIGURE 1. **Orbitrap MS analysis of the TgSkp1 glycopeptide.** RHΔΔ tachyzoites were lysed out of HFFs, urea-solubilized, and immunoprecipitated with bead-bound affinity-purified anti-TgSkp1 (pAb UOK75). The enriched preparation of TgSkp1 was eluted with triethylamine, reduced and alkylated, trypsinized, and analyzed by reverse phase-HPLC on an LTQ-XL Orbitrap MS. Extracted ion chromatograms showed coelution of a doubly charged (*m/z* 1436.6464) and a triply charged ion (*m/z* 958.0983) corresponding with a Δ mass of 0.56 ppm, to the predicted tryptic TgSkp1 peptide ^{145}IFNIVNDFT(HyP)EEEAQVR^{161} bearing a pentasaccharide with composition Hex3dHex1HexNAc1 (*A*). *B*, CID fragmentation of the doubly charged precursor ion yields a sequential loss of monosaccharide residues corresponding to Hex, Hex, dHex, Hex, and HexNAc, indicating the presence of a linear pentasaccharide. *C*, inspection of the full CID fragmentation spectrum shows b- (*blue* annotations) and y- (*red* annotations) ion series that match the predicted peptide sequence, as illustrated in the *inset*, and demonstrate that the glycan is linked via a hydroxylated derivative of Pro-154. Peptides with residual sugars are annotated in *green*.

TABLE 2

MS detection of Skp1 glycopeptides in strains

Isoforms of the Skp1 peptide ^{145}IFNIVNDFT**P**EEEAQVR were detected as described in Fig. 1. The distribution of raw ion counts among the detected isoforms are shown for the strains analyzed.

Strain	Expt #	Unmodified peptide			Hyp peptide			Hyp-HexNAc peptide			Hyp-penta-saccharide peptide		
		Occupancy*	*m/z***	ΔM (ppm)	Occupancy*	*m/z***	ΔM (ppm)	Occupancy*	*m/z***	ΔM (ppm)	Occupancy*	*m/z***	ΔM (ppm)
RHΔΔ	1	73%	1011.0002	-2.18	0%			0%			27%	1436.6464	-0.92
RHΔΔ	2	64%	1011.0052	2.77	0%			0%			35%	1436.6538	4.23
RHΔΔ/SF	1	78%	1011.0012	-1.19	0%			0%			22%	1436.6456	-1.48
RHphyAΔ-1	1	100%	1011.0018	-0.59	0%			0%			0%		
RHphyAΔ-1/SF	1	100%	1011.0044	1.98	0%			0%			0%		
RHgnt1Δ	1	60%	1010.9994	-2.97	40%	1018.9995	-0.35	0%			0%		
RHgnt1Δ	2	55%	1011.0024	0.00	45%	1019.0004	0.53	0%			0%		
RHpgtAΔ	1	72%	1011.0031	0.69	0%			28%	1120.5431	3.19	0%		

* apparent occupancy based on raw spectral counts.
** values refer to $[M+2H]^{2+}$ ions.

ion. The predominant ions were consistent with the presence of a linear pentasaccharide whose composition from the non-reducing end is Hex-Hex-dHex-Hex-HexNAc-. Fragmentation also yielded a series of a singly charged peptide and glycopeptide fragment b- and y-ions that confirmed the predicted amino acid sequence of the parent ion and demonstrated the position of the additional O atom as occurring on Pro (to yield Hyp) and the attachment of all sugars via Pro-154 (Fig. 1*C*). These data indicate that a fraction of Skp1 in *Toxoplasma* is modified by a linear pentasaccharide reminiscent of the linear pentasaccharide on DdSkp1.

Predicted TgSkp1-modifying Glycosyltransferases—BLASTP and TBLASTN searches for sequences corresponding to the three GT genes that catalyze formation of the pentasaccharide on DdSkp1 in ToxoDB (Version 7.3) yielded high scoring hits for DdGnt1 and DdPgtA. No candidates for a homolog of DdAgtA were detected using these algorithms or PSI- or PHI-BLAST toward either its catalytic or WD40 repeat domains. The *Toxoplasma* Dd*gnt1*-like sequence is represented by a one-exon gene model (Fig. 2*A*) in three sequenced strains of *Toxoplasma* (GT1, ME49, and VEG). The GT1 (type 1 strain) sequence (TGGT1_315885) exhibited 42% identity and 67% similarity to DdGnt1 over 214 amino acids of the ~250 amino acid catalytic domain (supplemental Fig. S1). Like DdGnt1, TGGT1_315885 is predicted to be a cytoplasmic protein because of the absence of detectable membrane or nuclear targeting motifs. However, at 1510 amino acids, TGGT1_315885 is substantially longer than DdGnt1 by 423 amino acids. As revealed by the amino acid sequence alignment (supplemental Fig. S1), and as illustrated in Fig. 2*C*, this results from multiple insertions throughout the length of the protein, a common occurrence in *Toxoplasma* genes as observed, *e.g.* in TgIF2Kb (19). In addition, a C-terminal sequence referred to as domain A that lies outside of the predicted catalytic domain (10) but is required for DdGnt1 activity is weakly conserved across these predicted proteins (Fig. 2). The remaining intervening sequences are poorly conserved even among coccidian apicomplexans that have PhyA-, Gnt1-, and PgtA-like sequences (supplemental Fig. S1). The coccidian *Sarcosystis neurona* is predicted to contain even longer insert sequences. In comparison, sequences from *Chromera velia* and *Vitrella brassicaformis*, representatives of the closest known photosynthetic relatives of apicomplexans in the alveolate superphylum (20), largely lack these inserts and resemble the length of the *Dictyostelium* sequence. Although the TgGnt1-coding region remains to be confirmed experimentally, two of the inserts are present in expressed sequence tags derived from mRNA, and a third was detected in a shotgun proteomics screen (Fig. 2*C*; supplemental Fig. S1). Although the significance of these additional sequences is enigmatic, their low conservation suggests that they fulfill *Toxoplasma*-specific functions that are unlikely to be related to the proposed enzymatic activity.

The *Toxoplasma* Dd*pgtA*-like sequence is represented by a 14-exon gene model (Fig. 2*B*). The predicted amino acid sequence of TGGT1_260650, from the type I GT1 strain, is 98 and 97% identical to that of the type II ME49 and type III VEG strain sequences, and the protein is predicted to be cytoplasmic. The *Toxoplasma* candidate is 1801 amino acids long, compared with the 768 amino acid length of DdPgtA, and the order of the two putative glycosyltransferase domains is reversed (Fig. 2*D*). The N-terminal CAZy GT2 family sequence of DdPgtA, which encodes a β3-GalT activity, has its sequence homolog in the C-terminal half of the *Toxoplasma* protein, whereas the C-terminal CAZy GT74 family sequence of DdPgtA, which encodes

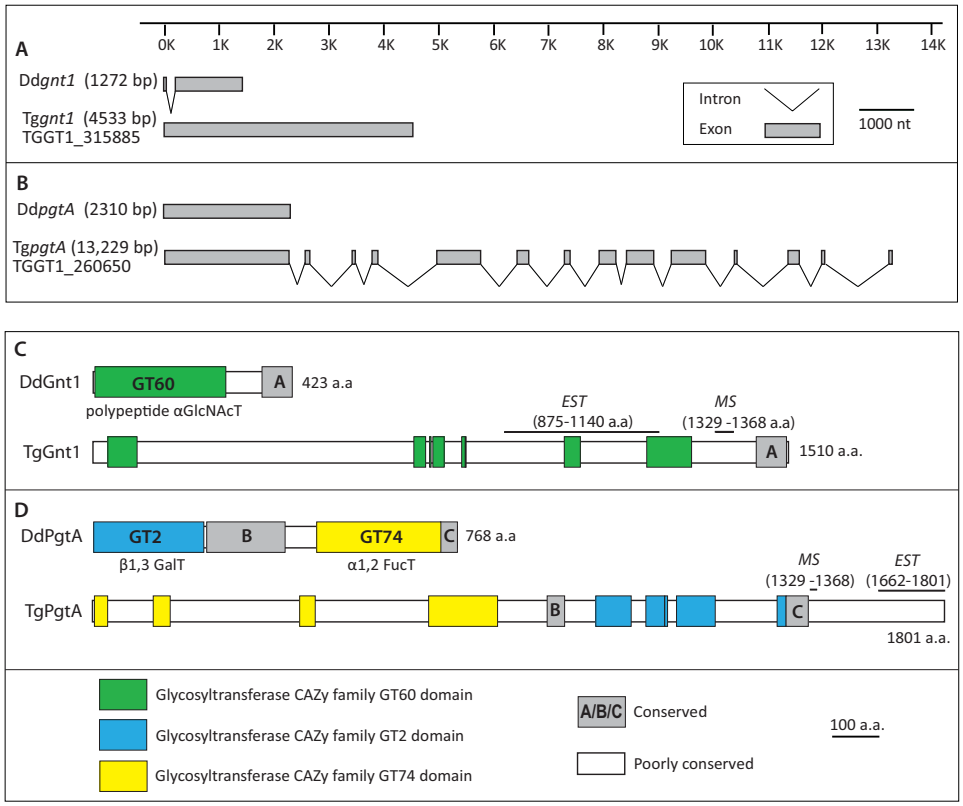

FIGURE 2. **Comparative genomic and domain organization of Gnt1 and PgtA from *Dictyostelium* and *Toxoplasma*.** *A* and *B*, exon-intron organization of the *gnt1* and *pgtA* genes. *gnt1* (*A*) and *pgtA* (*B*) gene models from *Dictyostelium discoideum* are from Refs. 8, 9 and available at dictybase.org (27). The gene models from *T. gondii* (GT1 (type 1) strain) are from Ref. 28. The length from the start codon to the stop codon in nucleotides is in *parentheses*. *C* and *D*, domain organization of Gnt1 (*C*) and PgtA (*D*) proteins. Gnt1- and PgtA-like sequences from *Toxoplasma* and three other coccidian apicomplexans were aligned with corresponding sequences from *D. discoideum* and three other amoebozoa, and sequences from two chromerid alveolates, as shown in supplemental Figs. S1 and S2. Regions of high conservation among all 10 sequences are shown in *color* for the glycosyltransferase-like sequences and in *gray* for non-GT-like sequences. *Toxoplasma* sequences whose expression has been confirmed at the transcriptional (expressed sequence tags) or proteomic (MS) level are indicated in Ref. 28. Diagrams are shown to scale.

an α2-FucT activity, has its homolog in the N-terminal half of the *Toxoplasma* protein. The GT2-like domain of the predicted TgPgtA is 22% identical and 60% similar to the DdPgtA-βGalT domain over the 191 most conserved amino acids, and the GT74-like domain is 33% identical and 66% similar to the DdPgtA-αFucT domain over 190 amino acids. The amino acid sequence alignment (supplemental Fig. S2) of the PgtA-like sequences reveal that, as for DdGnt1, the predicted apicomplexan PgtA-like sequences have numerous multiple inserts relative to the *Dictyostelium* prototype, as illustrated in Fig. 2*D*. These insert sequences, several of which occur in the protein based on expressed sequence tags and MS data (Fig. 2*D*), tend to diverge even within the coccidian apicomplexans and are minimal in the chromerids. Thus, they are unlikely to be critical for enzymatic activity.

Tggnt1 and TgpgtA Are Required for TgSkp1 Glycosylation—To determine whether Tg*gnt1* and Tg*pgtA* are involved in TgSkp1 glycosylation, their genes were disrupted by double-crossover homologous recombination in the RHΔΔ strain, as described under "Experimental Procedures" and illustrated in Fig. 3*A* for Gnt1. Deletion of *gnt1* in recovered clones was demonstrated by loss of a PCR product for *gnt1*-coding DNA, and positive PCRs for the insertion of the selection marker *hxgprt* between *gnt1*-flanking sequences, as described in Fig. 3*B*. To control for off-target genetic modifications, a *gnt1* disruption clone was complemented with a version of the original disruption DNA in which *hxgprt* was replaced by the deleted coding region and counter-selected for loss of *hxgprt* (Fig. 3*A*). The same set of PCRs was used to confirm the desired gene restoration in clonal isolates (Fig. 3*C*).

The effect of *gnt1* deletion on Skp1 glycosylation was evaluated initially by SDS-PAGE and Western blotting. As shown in Fig. 4*A*, Skp1 from parasites lacking *gnt1* (*lane 3*) migrated more rapidly than wild-type Skp1 (*lane 1*), and similarly to Skp1 from parasites whose *phyA* had been disrupted (*lane 2*). MS searches for the Skp1 glycopeptide were negative, but a novel hydroxypeptide corresponding to the hydroxylated but non-glycosylated Skp1 was obtained, in addition to the unmodified peptide (Table 2). Analysis of the complemented strain revealed that normal mobility of Skp1 in SDS-PAGE was at least partially restored. Thus, Skp1 HexNAcylation depends on Gnt1, and by analogy with the *Dictyostelium* example, Gnt1 is expected to directly catalyze addition of the first sugar in α-linkage onto Hyp154.

A similar analysis was performed on PgtA, whose genetic locus was manipulated as described in Fig. 3, *D–F*. In this case, a recently prepared genomic fosmid (13) was utilized to restore the genomic locus in the *pgtA*-disruption clone. Genomic DNA was utilized because of the large number of predicted introns and our difficulty in isolating a full-length cDNA using RT-PCR

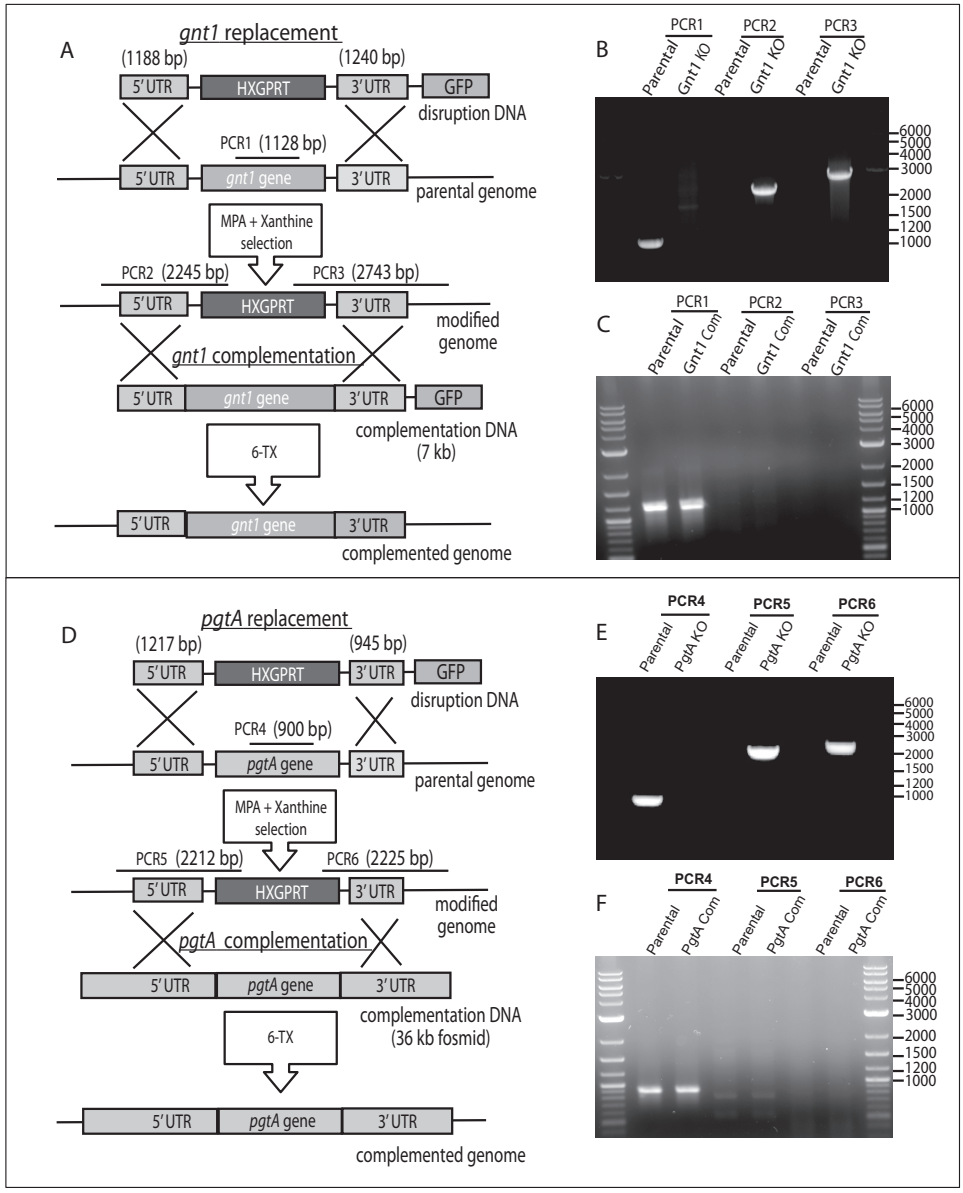

FIGURE 3. **Disruption and complementation of Tg*gnt1* and Tg*pgtA*.** *A*, strategy for deletion of Tg*gnt1* and its subsequent complementation. The plasmid-derived disruption of DNA with homologous targeting sequences was electroporated into parasites. Recovery of *hxgprt*-positive clones that were resistant to MPA and xanthine and were GFP-negative were candidates for double crossover gene replacement. *B*, gene replacement was confirmed by PCR-1, which demonstrated loss of *gnt1* coding DNA, and PCR-2 and -3, which demonstrated that the inserted *hxgprt* DNA was flanked by neighboring *gnt1* DNA. To complement Tg*gnt1* in the disruption strain, a plasmid containing an ~7-kb genomic locus, including Tg*gnt1* coding region and 5′- and 3′-untranslated regions (*A*), was transfected. Complemented strains where the *hxgprt* is replaced by Tg*gnt1* locus were counter-selected under 6-thioxanthine. *C*, *gnt1* replacement was confirmed by the positive PCR-1 and negative reactions for PCR-2 and PCR-3, which depended on the presence of *hxgprt*. *D–F*, Tg*pgtA* was similarly targeted for disruption and complementation. Characteristics of the above strains are summarized in Table 1.

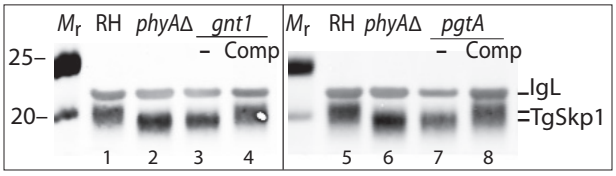

FIGURE 4. **Disruption of Tg*gnt1* or Tg*pgtA* affects TgSkp1 glycosylation.** Soluble S16 fractions from equivalent numbers (3×10^6 cells) of parental RHΔΔ (RH) and RH*phyA*Δ-1 (*phyA*$^-$), RH*gnt1*Δ, RH*pgtA*Δ, and their complemented cells were resolved by 4–12% SDS-PAGE, electroblotted, and probed using anti-TgSkp1 (UOK75) antiserum. Changes in glycosylation inferred from altered gel mobility were confirmed by mass spectrometry (Table 2). Similar results were obtained for independently derived clones of RH*gnt1*Δ and RH*pgtA*Δ.

(data not shown), and the fosmid clone was used because of the predicted large size (13.2 kb) of its genomic locus. As shown in Fig. 4, *lane 7*, Skp1 glycosylation also appeared to be affected by the loss of *pgtA* based on SDS-PAGE/Western blotting, and this was confirmed by the accumulation of the HexNAc form of Skp1, the expected acceptor substrate of PgtA, based on MS analysis of tryptic peptides (Table 2). As expected, restoration of the *pgtA* locus resulted in at least partial recovery of Skp1 glycosylation (Fig. 4, *lane 8*). At a minimum, PgtA is thus required for addition of the second sugar to the Skp1 glycan.

TgGnt1 Has Properties of a Skp1 Polypeptide UDP-GlcNAc:HO-Skp1 GlcNAcT—A previous study detected a Gnt1-like activity in tachyzoite cytosolic extracts, based on transfer of ^{3}H

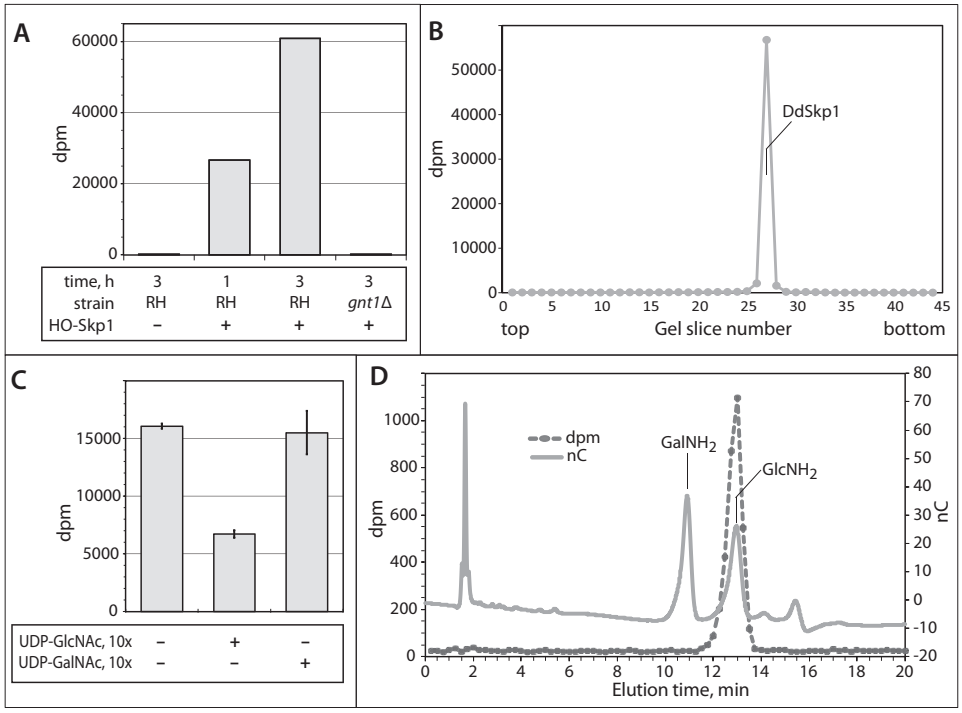

FIGURE 5. **TgGnt1 is a Skp1 GlcNAcT.** *A*, GlcNAcT activity in S100 cytosolic parasite was assayed based on transfer of ^{3}H from 0.5 μM UDP-[^{3}H]GlcNAc to exogenous HO-DdSkp1 for 1–3 h as described under "Experimental Procedures." Reactions were loaded onto and separated on an SDS-polyacrylamide gel, and the Coomassie Blue-stained DdSkp1 bands were excised and subjected to liquid scintillation spectroscopy. The reaction time, presence of HO-Skp1, and source of the extract (RHΔΔ or RH, or RH*gnt1*Δ or *gnt1*Δ) were varied as indicated. *B*, entire lane from a parallel 3-h reaction (RH, +HO-Skp1) from *A* was analyzed for incorporation of ^{3}H. Incorporation was only detected at the migration position of DdSkp1. *C*, donor substrate specificity of the GlcNAcT activity was examined by including a 9-fold excess of unlabeled UDP-GlcNAc or UDP-GalNAc to reactions containing 10 μM UDP-[^{3}H]GlcNAc. Incorporation was measured as in *A*. *Error bars* show standard deviations of the mean of two replicates from each of two independent reactions. *D*, analysis of incorporated ^{3}H. The reacted Skp1 band was excised from a PVDF membrane electroblot of the SDS-polyacrylamide gel, subjected to acid hydrolysis in 6 N HCl, and analyzed by high pH anion exchange chromatography. The hydrolysate was supplemented with $GlcNH_2$ and $GalNH_2$ and chromatographed on a Dionex PA-1 column. Elution of the sugar standards was monitored by a pulsed amperometric detector (*nC*), and fractions were collected to monitor the elution of ^{3}H by scintillation counting (dpm).

from UDP-[^{3}H]GlcNAc to $DdHis_{10}$-Skp1 that was recovered from an SDS-polyacrylamide gel (21). This activity depended on addition of DdPhyA indicating dependence on Hyp. Replication of an optimized form of this assay (see "Experimental Procedures") revealed time-dependent transfer of ^{3}H to HO-DdSkp1 that was absent from *gnt1*Δ extracts (Fig. 5*A*). As shown in Fig. 5*B*, no incorporation into endogenous proteins was detected based on analysis of an entire SDS-polyacrylamide gel lane, indicating absence of activity of endogenous GTs from other sources, such as the Golgi, that modify other targets in these cytosolic preparations. The lack of other radiolabeled proteins is inconsistent with the existence of an intermediate TgGnt1 substrate that itself mediates modification of Skp1. Incorporation was reduced as expected after addition of a 10-fold excess of unlabeled UDP-GlcNAc, but not of unlabeled UDP-GalNAc (Fig. 5*C*), indicating that the enzyme is selective for the GlcNAc isomer. Because a homolog of Gnt1 that resides in the Golgi transfers GalNAc to proteins (22), and *Toxoplasma* possesses an epimerase that can interconvert UDP-GlcNAc with UDP-GalNAc, the nature of the transferred ^{3}H was confirmed by another method. ^{3}H was found to be incorporated as GlcNAc, based on co-chromatography of ^{3}H released by HCl hydrolysis, which de-*N*-acetylates GlcNAc to $GlcNH_2$, with a $GlcNH_2$ standard (Fig. 5*D*). Although the evidence that TgGnt1 modifies Skp1 in this assay is indirect, its homology with DdGnt1, whose purified recombinant version can αGlcNAcylate HO-DdSkp1 *in vitro* (8), suggests that TgGnt1 also directly αGlcNAcylates TgSkp1.

TgPgtA Is a Bifunctional Glycosyltransferase with GalT and FucT Activities—To characterize the role of *pgtA* in extending the Skp1 glycan, the above assay was first modified by substituting UDP-[^{3}H]Gal for UDP-[^{3}H]GlcNAc and GlcNAc-Skp1 for HO-Skp1. Time-dependent incorporation of ^{3}H into GlcNAc-Skp1 was observed (Fig. 6*A*). Incorporation into the Skp1 band on the SDS-polyacrylamide gel required the inclusion of Skp1, and Skp1 was the only protein that incorporated detectable radioactivity (Fig. 6*B*). No incorporation was detected in extracts of *pgtA*Δ cells. Recovery and analysis of the ^{3}H after acid hydrolysis confirmed incorporation as Gal rather than a derivative (Fig. 6*C*). Similar findings were observed in a corresponding FucT assay, in which UDP-[^{3}H]Gal was replaced by GDP-[^{3}H]Fuc (Fig. 6, *D–F*). However, incorporation of ^{3}H depended on the inclusion of UDP-Gal (unlabeled), in contrast to the GalT reaction that did not require GDP-Fuc (Fig. 6*A*). This indicated that TgPgtA is, like DdPgtA (9), a processive diglycosyltransferase that catalyzes the sequential addition of Gal and then Fuc, an order consistent with the MS-MS data. Although >95% of incorporation of [^{3}H]Fuc into the Skp1 band depended on Skp1 and *pgtA* (Fig. 6, *D* and *E*), residual incorporation was observed at this

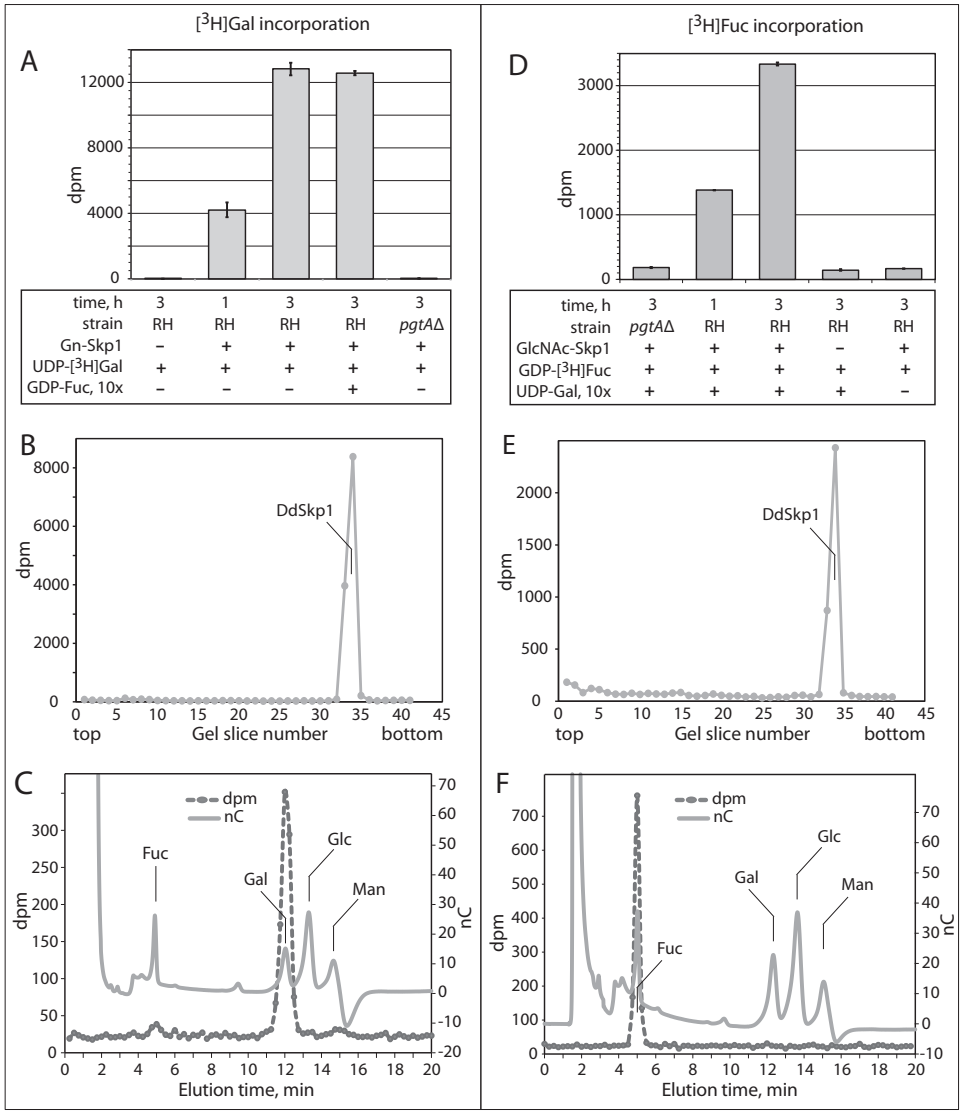

FIGURE 6. **PgtA is a Skp1 GalT and FucT.** *A*, GalT activity directed toward GlcNAc-Skp1 was assayed as described for GlcNAcT activity in Fig. 5*A*, except that GlcNAc-Skp1 and UDP-[^{3}H]Gal were used in place of HO-Skp1 and UDP-[^{3}H]GlcNAc. The reaction time, inclusion of GlcNAc-Skp1 and GDP-Fuc, and source of the extract (RHΔΔ or RH, or RH*pgtA*Δ or *pgtA*Δ) were varied as indicated. *B*, entire lane from a parallel 3-h reaction (RH, +Gn-Skp1) from *A* was analyzed for incorporation of ^{3}H. Incorporation was only detected at the migration position of DdSkp1. *C*, [^{3}H]DdSkp1 from the 3-h GalT reaction in *A* was isolated as in Fig. 5*D* and hydrolyzed in 4 M TFA. The hydrolysate was chromatographed on a Dionex PA-1 column with internal standards of Gal, Glc, Man, and Fuc, and the elution of ^{3}H was monitored by scintillation counting of collected fractions. *D–F*, FucT activity assays. Reactions were conducted as above except that GDP-[^{3}H]Fuc replaced UDP-[^{3}H]Gal, and the dependence of incorporation on a 10-fold concentration excess of UDP-Gal, GlcNAc-Skp1, and PgtA in the extract and time was examined.

position and elsewhere in the gel indicative of additional *pgtA*- and Skp1-independent FucT activity in the extract. These results are consistent with accumulation of GlcNAc-Skp1 and the absence of higher glycosylation states in *pgtA*Δ cells (Fig. 4 and Table 2).

TgGnt1 and TgPgtA Are Important for Toxoplasma Growth in Cell Culture—Previous studies revealed that disruption of exon 1 of *phyA* results in a parasite growth defect, which could be detected as reduced plaque areas after 5 days of replication on a fibroblast monolayer (5). To check that no residual *phyA* activity was present, all nine exons were deleted (RH*phyA*Δ-2). A similarly reduced ability to grow on monolayers was observed, as illustrated in Fig. 7*A* and quantified in *B*. Furthermore, deletion of exon 1 in a strain in which Skp1 was C-terminally modified with an SF-epitope tag, which itself did not affect growth, also resulted in slowed growth (Fig. 7*C*). To examine the roles *gnt1* and *pgtA*, the plaque-forming abilities of the disruption strains described above were analyzed. As shown in Fig. 7*B*, *gnt1*Δ cells exhibited slow growth that was statistically indistinguishable from that of *phyA*Δ cells. *pgtA*Δ cells also exhibited a slow growth phenotype, which was intermediate between that of *gnt1*Δ and parental (RHΔΔ) cells. Complementation of *gnt1* and *pgtA* by gene replacement at their original loci restored normal growth (Fig. 7*D*), showing that the growth differences in the original disruption strains could be attributed to the GT targets. Although these findings do not demonstrate directly that the altered modifications of Skp1 are involved in reduced growth, the finding that three independent enzymes that share Skp1 as a target substrate exhibit a similar deficiency is consistent

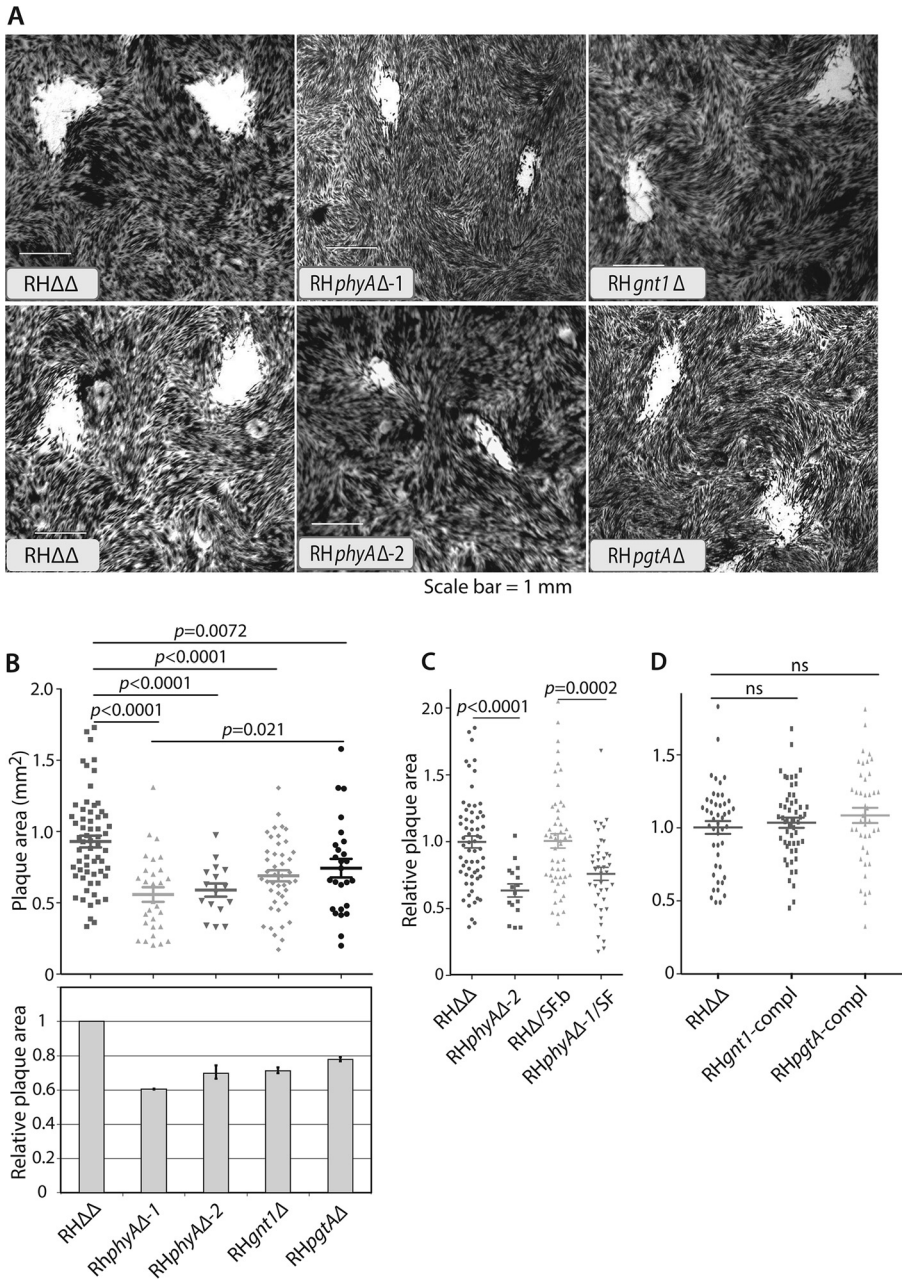

FIGURE 7. **Role of Tg*gnt1* and Tg*pgtA* in parasite proliferation.** HFF monolayers were inoculated with freshly isolated tachyzoite stage parasites at a multiplicity of infection of 0.002. After 5.5 days, monolayers were stained with crystal violet. *A*, representative images of cleared areas of the host monolayers. *B–D*, images digitized and plaque areas were calculated. The dot plots show the area distributions and average values ± S.E. from a representative of two independent experiments. Average parental strain areas ranged from 0.5 to 1.0 mm^2. *p* values for statistical significance of the differences, based on a one-way analysis of variance test, are shown above. *ns* = not significant. *B*, data from RHΔΔ, RH*phyA*Δ-1, and RH*phyA*Δ-2, generated by different strategies, RH*gnt1*Δ, and RH*pgtA*Δ strains. *Bar graph* shows average (±S.D.) from two independent experiments. *C*, data from strains in which Skp1 was SF-tagged. *D*, data from Tg*gnt1* or Tg*pgtA* complemented (*compl*) strains.

with a role for Skp1, a model that has both biochemical and genetic support in *Dictyostelium*.

Discussion

Skp1 isolated from the tachyzoite stage of *Toxoplasma* is partially modified by a glycan chain that consists of five sugars and is linked to the hydroxylated form of Pro-154. The monosaccharides are organized as a linear pentasaccharide with a sequence, reading from the peripheral non-reducing end, of Hex-Hex-α Fuc-β Gal-α GlcNAc-, based on mass spectrometry and characterization of the core GTs. Remarkably, these properties match those of the glycan that was previously characterized on Skp1 from an unrelated protist, the social amoeba *Dictyostelium* (6). Genetic disruption of glycosylation rendered a growth defect in host cell monolayers, implicating a role for *Toxoplasma* $E3^{SCF}$ ubiquitin ligases in cell proliferation.

The predicted Skp1 glycan was analyzed at the glycopeptide level because of the resistance of the glycan-Hyp linkage to known methods of cleavage. Native Skp1 from parasites was analyzed to avoid overexpression artifacts, but this necessitated

application of highly sensitive methods due to the limited amount of material available because *Toxoplasma* can only be grown intracellularly. As is typical for the analysis of glycopeptides by mass spectrometry, their detection required manual inspection of spectra for candidate ions, because of suppression and abundance issues. The pentasaccharide peptide was detected in an exhaustive search of the primary spectra for tryptic peptides bearing Pro-154 (Fig. 1), the previously documented hydroxylation site (5), and any combination of up to eight monosaccharides. Decomposition analysis in the gas phase confirmed the glycan's location at Hyp154 and suggested that it is organized as a linear pentasaccharide with a sequence, from the non-reducing end, of Hex-Hex-dHex-Hex-HexNAc-. The only other peptide isoform detected was non-hydroxylated and therefore non-glycosylated (Table 2), suggesting limited glycosylation microheterogeneity.

The sugar identities were investigated by highly sensitive incorporation of radioactive sugars mediated by parasite extracts that harbor the biosynthetic enzymes. Cytosolic extracts were observed to specifically incorporate radioactivity from three different radioactive sugar nucleotides into recombinantly generated isoforms of *Dictyostelium* Skp1, which was previously shown to be an excellent substrate for DdPhyA (5). Based on the confirmed identities of the ^{3}H-sugars after incorporation, the core trisaccharide is concluded to consist of Fuc-Gal-GlcNAc, which matches the dHex-Hex-HexNAc- found by MS.

Incorporation of [^{3}H]GlcNAc into HO-Skp1 depended on Tg*gnt1* based on the absence of activity in *gnt1*Δ extracts (Fig. 5). By analogy with its *Dictyostelium* ortholog, TgGnt1 is inferred to transfer GlcNAc in an α-linkage to Hyp154 of TgSkp1. Incorporation of [^{3}H]Gal depended on Tg*pgtA* (Fig. 6), and the addition of [^{3}H]Fuc, which also depended upon Tg*pgtA*, required prior addition of Gal (Fig. 6). These linkages require further study to determine whether they are conserved with the *Dictyostelium* example. Thus, although the physical order of the two GT domains is reversed relative to DdPgtA (Fig. 2), the order of addition of the two sugars is conserved. The existence of the two terminal Hex residues was unexpected because of the absence of a homolog for AgtA in the *Toxoplasma* genome, and their identities are under current investigation.

Both Tg*gnt1* and Tg*pgtA* were important for efficient plaque-forming ability in tissue culture monolayers cultivated under standard conditions (Fig. 7). Loss of *gnt1* was as severe as loss of *phyA*, the prolyl 4-hydroxylase that is required for Gnt1 action on Skp1. Loss of *pgtA* resulted in an intermediate effect, *i.e.* the plaque-forming ability was improved relative to cells lacking *phyA*. These effects were specific for the GT genes as normal plaque-forming ability was restored upon genetic complementation to the original genotype. Thus, Gnt1 appears to make a major contribution to *phyA*-dependent growth, but complete realization appears to depend on Gnt1-dependent glycosylation contributed by, at least on Skp1, PgtA and the additional unknown GTs. In *Dictyostelium*, biochemical studies indicate that Skp1 is the only substrate for the orthologs of these GTs, and disruption of either *gnt1* or *pgtA* inhibits development in a way that is related to, but less severe than, disruption of *phyA* (10). Gene dosage manipulations on Skp1 expression show inverse effects on development consistent with the modification genes acting via Skp1 in this organism, a model that is supported by point mutations that remove the target Pro residue, and from a double mutant between a GT gene and one of two Skp1 genes (23). By analogy, and based on similar phenotypes of Tg*phyA*Δ and Tg*gnt1*Δ, we propose that the modification genes render their effects in a common pathway that affects Skp1. Further studies on Skp1 itself are needed to evaluate this possibility.

The reduced plaque areas are consistent with a role for Skp1 modification in cell cycle progression as demonstrated in yeast and mammalian cells, where SCF-type E3 ubiquitin ligases are important for signaling proteasome-dependent turnover of cell cycle kinase inhibitors (24). However, SCF ligases represent a family of enzymes that includes many F-box proteins with distinct substrate receptor activities (25). Given the large variety of substrates known to be recognized by yeast, plant, and human F-box proteins, further studies are needed to evaluate whether other processes required for plaque formation, such as binding of the parasite to host cells, ingress and/or egress are affected. In future studies, it will be interesting to evaluate whether any of these potential mechanisms are more severely affected in low O_2 or altered metabolic states that are anticipated to influence Skp1 modification enzyme activities in cells (11).

PhyA-, Gnt1-, and PgtA-like sequences are selectively conserved across a broad spectrum of unicellular eukaryotes, including representatives of all major protist clades (6). Validation of their shared functions in both *Toxoplasma* and *Dictyostelium*, which are highly diverged, suggests that Skp1 hydroxylation and glycosylation occurred in ancestral eukaryotes prior to their loss in fungi, higher plants, animals, and select protists. The relatively rapid evolution of F-box proteins, with which Skp1 partners for many if not all of its functions, suggests that Skp1 modifications serve an outsized role in environmental regulation of unique lineage and species-specific functions in many unicellular organisms.

Author Contributions—K. R. conducted most of the experiments, analyzed the results, assembled the figures, and wrote most of the first draft. P. Z. conducted the mass spectrometry and interpreted the data together with L. W. M. M. and H. vdW. contributed to the enzymatic assays and HPAEC analyses. I. J. B. and C. M. W. conceived the ideas and the experimental strategies for the project. C. M. W. wrote the final draft.

Acknowledgments—We thank Drs. Boris Striepen, Gustavo Arrizabalaga, and Vern Carruthers for the gifts of plasmids.

References

1. Kim, K., and Weiss, L. M. (2004) *Toxoplasma gondii*: the model apicomplexan. *Int. J. Parasitol.* **34,** 423–432
2. Pereira-Chioccola, V. L., Vidal, J. E., and Su, C. (2009) *Toxoplasma gondii* infection and cerebral toxoplasmosis in HIV-infected patients. *Future Microbiol.* **4,** 1363–1379
3. Luft, B. J., and Remington, J. S. (1992) Toxoplasmic encephalitis in AIDS. *Clin. Infect. Dis.* **15,** 211–222
4. Lambert, H., and Barragan, A. (2010) Modelling parasite dissemination: host cell subversion and immune evasion by *Toxoplasma gondii*. *Cell.*

Microbiol. **12,** 292–300
5. Xu, Y., Brown, K. M., Wang, Z. A., van der Wel, H., Teygong, C., Zhang, D., Blader, I. J., and West, C. M. (2012) The Skp1 protein from *Toxoplasma* is modified by a cytoplasmic prolyl 4-hydroxylase associated with oxygen sensing in the social amoeba *Dictyostelium. J. Biol. Chem.* **287,** 25098–25110
6. West, C. M., Wang, Z. A., and van der Wel, H. (2010) A cytoplasmic prolyl hydroxylation and glycosylation pathway modifies Skp1 and regulates O_2-dependent development in *Dictyostelium. Biochim. Biophys. Acta* **1800,** 160–171
7. Schafer, C. M., Sheikh, M. O., Zhang, D., and West, C. M. (2014) Novel regulation of Skp1 by the *Dictyostelium* AgtA α-galactosyltransferase involves the Skp1-binding activity of its WD40 repeat domain. *J. Biol. Chem.* **289,** 9076–9088
8. van der Wel, H., Morris, H. R., Panico, M., Paxton, T., Dell, A., Kaplan, L., and West, C. M. (2002) Molecular cloning and expression of a UDP-*N*-acetylglucosamine (GlcNAc):hydroxyproline polypeptide GlcNAc-transferase that modifies Skp1 in the cytoplasm of *Dictyostelium*. *J. Biol. Chem.* **277,** 46328–46337
9. van der Wel, H., Fisher, S. Z., and West, C. M. (2002) A bifunctional diglycosyltransferase forms the Fucα1,2Galβ1,3-disaccharide on Skp1 in the cytoplasm of *Dictyostelium. J. Biol. Chem.* **277,** 46527–46534
10. Zhang, D., van der Wel, H., Johnson, J. M., and West, C. M. (2012) The Skp1 prolyl 4-hydroxylase of *Dictyostelium* contributes glycosylation-independent and -dependent effects on O_2-dependent development without affecting Skp1 stability. *J. Biol. Chem.* **287,** 2006–2016
11. West, C. M., and Blader, I. J. (2015) Oxygen sensing by protozoans: How they catch their breath. *Curr. Opin. Microbiol.* **26,** 41–47
12. Sheikh, M. O., Xu, Y., van der Wel, H., Walden, P., Hartson, S. D., and West, C. M. (2015) Glycosylation of Skp1 promotes formation of Skp1-Cullin-1-F-box protein complexes in *Dictyostelium. Mol. Cell. Proteomics* **14,** 66–80
13. Vinayak, S., Brooks, C. F., Naumov, A., Suvorova, E. S., White, M. W., and Striepen, B. (2014) Genetic manipulation of the *Toxoplasma gondii* genome by fosmid recombineering. *MBio* **5,** e02021
14. Huynh, M. H., and Carruthers, V. B. (2009) Tagging of endogenous genes in a *Toxoplasma gondii* strain lacking Ku80. *Eukaryot. Cell* **8,** 530–539
15. Figueras, M. J., Martin, O. A., Echeverria, P. C., de Miguel, N., Naguleswaran, A., Sullivan, W. J., Jr., Corvi, M. M., and Angel, S. O. (2012) *Toxoplasma gondii* Sis1-like J-domain protein is a cytosolic chaperone associated to HSP90/HSP70 complex. *Int. J. Biol. Macromol.* **50,** 725–733
16. Kimmel, J., Smith, T. K., Azzouz, N., Gerold, P., Seeber, F., Lingelbach, K., Dubremetz, J. F., and Schwarz, R. T. (2006) Membrane topology and transient acylation of *Toxoplasma gondii* glycosylphosphatidylinositols. *Eukaryot. Cell* **5,** 1420–1429
17. Teng-Umnuay, P., van der Wel, H., and West, C. M. (1999) Identification of a UDP-GlcNAc:Skp1-hydroxyproline GlcNAc-transferase in the cytoplasm of *Dictyostelium*. *J. Biol. Chem.* **274,** 36392–36402
18. Sheikh, M. O., Schafer, C. M., Powell, J. T., Rodgers, K. K., Mooers, B. H., and West, C. M. (2014) Glycosylation of Skp1 affects its conformation and promotes binding to a model F-box protein. *Biochemistry* **53,** 1657–1669
19. Narasimhan, J., Joyce, B. R., Naguleswaran, A., Smith, A. T., Livingston, M. R., Dixon, S. E., Coppens, I., Wek, R. C., and Sullivan, W. J., Jr. (2008) Translation regulation by eukaryotic initiation factor-2 kinases in the development of latent cysts in *Toxoplasma gondii. J. Biol. Chem.* **283,** 16591–16601
20. Moore, R. B., Oborník, M., Janouskovec, J., Chrudimský, T., Vancová, M., Green, D. H., Wright, S. W., Davies, N. W., Bolch, C. J., Heimann, K., Slapeta, J., Hoegh-Guldberg, O., Logsdon, J. M., Carter, D. A. (2008) A photosynthetic alveolate closely related to apicomplexan parasites. *Nature* **451,** 959–963
21. West, C. M., van der Wel, H., and Blader, I. J. (2006) Detection of cytoplasmic glycosylation associated with hydroxyproline. *Methods Enzymol.* **417,** 389–404
22. Wojczyk, B. S., Stwora-Wojczyk, M. M., Hagen, F. K., Striepen, B., Hang, H. C., Bertozzi, C. R., Roos, D. S., and Spitalnik, S. L. (2003) cDNA cloning and expression of UDP-*N*-acetyl-D-galactosamine:polypeptide *N*-acetylgalactosaminyltransferase T1 from *Toxoplasma gondii*. *Mol. Biochem. Parasitol.* **131,** 93–107
23. Wang, Z. A., Singh, D., van der Wel, H., and West, C. M. (2011) Prolyl hydroxylation- and glycosylation-dependent functions of Skp1 in O_2-regulated development of *Dictyostelium*. *Dev. Biol.* **349,** 283–295
24. Willems, A. R., Schwab, M., and Tyers, M. (2004) A hitchhiker's guide to the cullin ubiquitin ligases: SCF and its kin. *Biochim. Biophys. Acta* **1695,** 133–170
25. Skaar, J. R., Pagan, J. K., and Pagano, M. (2013) Mechanisms and function of substrate recruitment by F-box proteins. *Nat. Rev. Mol. Cell Biol.* **14,** 369–381
26. Fox, B. A., Ristuccia, J. G., Gigley, J. P., and Bzik, D. J. (2009) Efficient gene replacements in *Toxoplasma gondii* strains deficient for nonhomologous end joining. *Eukaryot. Cell* **8,** 520–529
27. Basu, S., Fey, P., Jimenez-Morales, D., Dodson, R. J., and Chisholm, R. L. (2015) DictyBase 2013: integrating multiple Dictyostelid species. *Genesis* **53,** 523–534
28. Gajria, B., Bahl, A., Brestelli, J., Dommer, J., Fischer, S., Gao, X., Heiges, M., Iodice, J., Kissinger, J. C., Mackey, A. J., Pinney, D. F., Roos, D. S., Stoeckert, C. J., Jr., Wang, H., and Brunk, B. P. (2008) ToxoDB: an integrated *Toxoplasma gondii* database resource. *Nucleic Acids Res.* **36,** D553–D556